

ANALYSIS OF THE PHASE TRANSITIONS AT HIGH TEMPERATURE IN Sr₂NaNb₅O₁₅ CERAMIC BY IMPEDANCE SPECTROSCOPY

D. H. M. Gênova*; S. A. Dantas; M. A. L. Nobre; S. Lanfredi
Faculdade de Ciências e Tecnologia – FCT
Universidade Estadual Paulista – UNESP
Departamento de Física, Química e Biologia – DFQB
Laboratório de Compósitos e Cerâmicas Funcionais – LaCCeF
R. Roberto Simonsen 305, C. P. 467, Presidente Prudente, SP 19060-900
**genovadh@gmail.com*

ABSTRACT

Oxide materials with tetragonal tungsten bronze-TTB type structure are of great scientific and technical-industrial interest as materials for laser modulation and frequency multiplicity, and generation of second-harmonic for application in pyroelectric detectors, piezoelectric and electrooptic devices and memories. In this work were investigated the dielectric properties of the Sr₂NaNb₅O₁₅ ceramic prepared by poliol modified method. The dielectric characterization was realized by impedance spectroscopy since room temperature up to 680 °C, in the frequency range from 500 mHz to 13 MHz. The permittivity curve of Sr₂NaNb₅O₁₅ shows a polarization peak of high intensity at around 242 °C, with a permittivity value equal to 1650 assigned to the Curie's temperature. A second maximum at low intensity and diffuse is observed between room temperature and 170 °C, attributed to the structural phase transitions. Phenomena of phase transitions in the permittivity curve of Sr₂NaNb₅O₁₅ as a function of temperature is discussed.

Key-words: niobate, impedance spectroscopy, dielectric permittivity, phase transition, tetragonal tungsten bronze.

INTRODUCTION

Niobates with tetragonal tungsten bronze (TTB) type structure are of great scientific and technical-industrial interest as materials for laser modulation and frequency multiplicity, and generation of second-harmonic for application in pyroelectric detectors and piezoelectric transducers ⁽¹⁾. Some polycation ferroelectric oxides are also important due to the potential microwave telecommunications progress involving satellite broadcasting and related devices ⁽²⁾. Furthermore, these materials have the potential to replace, in some cases, members of the classic set of ferroelectric ceramics, such as $\text{Pb}(\text{Zr,Ti})\text{O}_3$ (PZT), $[(\text{Pb}(\text{Mg}_{1/3}\text{Nb}_{2/3})\text{O}_3)]$ (PMN), and $[(\text{Pb,L a})(\text{Zr,Ti})\text{O}_3]$ (PLZT) ⁽³⁾. In the last years, alkaline and alkaline earth niobates with TTB-type structure, such as $\text{KSr}_2\text{Nb}_5\text{O}_{15}$, $\text{NaSr}_2\text{Nb}_5\text{O}_{15}$, $\text{KBa}_2\text{Nb}_5\text{O}_{15}$, $\text{NaBa}_2\text{Nb}_5\text{O}_{15}$, and $\text{K}_3\text{Li}_2\text{Nb}_5\text{O}_{15}$, have proved to be of interest due to the high anisotropy of their crystalline structure ⁽⁴⁾. The TTB structure can be considered as a derivative of the classical perovskite structure. It can be described by the chemical formula $(A1)_2(A2)_4C_4\text{Nb}_{10}\text{O}_{30}$. A1, A2, and C denote different sites of oxygen atom coordination in the crystal structure. The A1 cavities have a cuboctahedral coordination, the A2 cavities, pentacapped pentagonal prismatic coordination, and the C cavities, tricapped trigonal prismatic coordination. Cavity size decreases in the following order: $A2 > A1 > C$.

Figure 1 shows the representation of the tetragonal tungsten bronze TTB-type structure of $\text{Sr}_2\text{NaNb}_5\text{O}_{15}$.

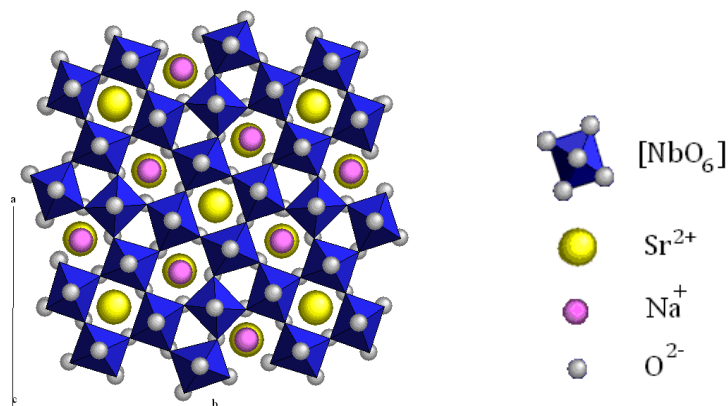


Figure 1- Representation of the tetragonal tungsten bronze TTB-type structure of $\text{Sr}_2\text{NaNb}_5\text{O}_{15}$.

In TTB-type compounds, alkaline and/or alkaline-earth metals, are located in the A1 and A2 sites, while only small cations like Li are found in the C site ⁽⁵⁾. Taking into account the TTB-type structure, a wide variety of cation substitution is possible. In a broad sense, TTB-type compounds with $A_6Nb_{10}O_{30}$ formula, being $A = Sr, Ba$, are semiconductor oxides containing niobium ions. In a TTB-type structure, the coexistence of cations is favorable in both tetragonal and pentagonal sites. In some, the cation repartition disorder has been correlated to the relaxor behavior ⁽⁶⁾. Among TTB-type oxides, the classical ferroelectric quaternary niobates are of particular relevance. The size and type of replacement of ions in different sites of the structure and the degree of disorder have a significant effect on the dielectric properties of these materials.

In this work was investigated the dielectric behavior of the $Sr_2NaNb_5O_{15}$ ceramic with TTB-type structure synthesized by Modified Polyol method. The dielectric characterization was carried out by impedance spectroscopy.

EXPERIMENTAL PROCEDURE

Nanostructured $Sr_2NaNb_5O_{15}$ single phase powder was synthesized by the Modified Polyol method. As a whole, this method gives rise a better control of reagents, a low calcination temperature, a single phase material and powder with high specific surface area. The starting reagents for the powder synthesis via chemical route were nitric acid HNO_3 (99.5% Reagen), strontium carbonate $SrCO_3$ (99.0% Reagen), sodium carbonate Na_2CO_3 (99.0% Reagen), ethylene glycol $HOCH_2CH_2OH$ (98.0% Synth) and niobium ammonium oxalate $NH_4H_2[NbO(C_2O_4)_3] \cdot 3H_2O$ (CBMM-Brazil). All salts were dissolved in nitric acid with continuous stir in a beaker. In the sequence, 100 ml of ethylene glycol was added. The solution was heated at 90 °C, promoting the decomposition of NO_3 group, similar to the process developed in the Pechini method ^(7, 8). After the polyesterification reaction, a polymeric gel is obtained. The polymer is maintained in the beaker undergoes a primary calcinations in a furnace type box. The heating cycle was carried out via two calcinations steps, in N_2 atmosphere with flux of 500 ml/min. From room temperature, the temperature was increased using a heating rate equal to 10 °C/min up to 150 °C at this point the temperature was kept constant during 30

min. In the sequence, the same heating rate was used to increase the temperature at 300 °C, being maintained during 1 hour. After this cycle, the furnace was cooling to the natural rate. The nitrogen flux was constant at 500 ml/min during the cooling cycle. This process leads to the partial polymer decomposition forming a resin, which consist in a brittle reticulated material. This material was deagglomerate in an agate mortar being termed precursor. The precursor was calcinated in a tube furnace in oxygen atmosphere. The time and temperature parameters, of the precursor powder, were optimized to obtain $\text{Sr}_2\text{NaNb}_5\text{O}_{15}$ single phase powders with high crystallinity. The calcinations was carried out in the temperatures range from 350 to 1150 °C during 12 hours, using heating rate equal to 5 °C/min, with oxygen flux of 300 ml/min.

Figure 2 shows the fluxogram of preparation of the $\text{Sr}_2\text{NaNb}_5\text{O}_{15}$ powder from Modified Polyol method.

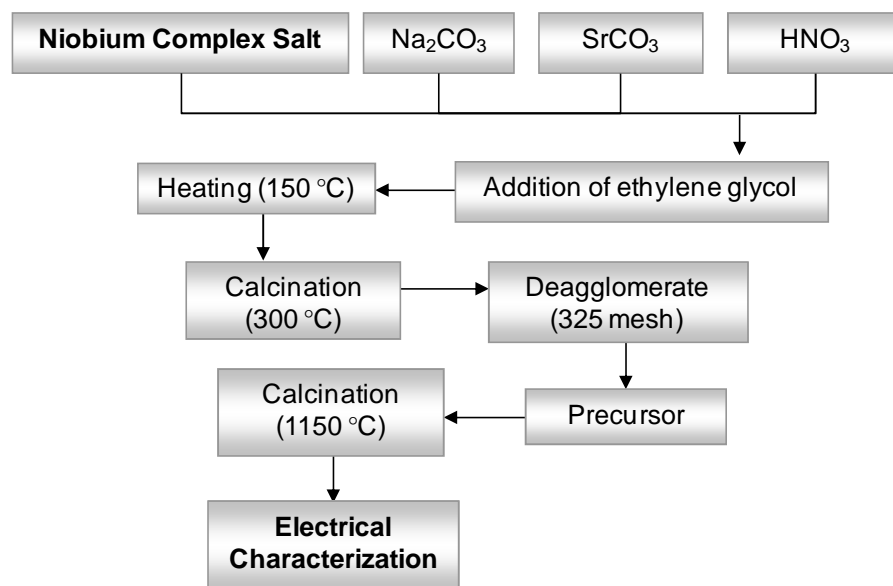


Figure 2. Fluxogram of preparation of the $\text{Sr}_2\text{NaNb}_5\text{O}_{15}$ powder from Modified Polyol method.

In the sequence, the powder was uniaxially pressed into pellet form. The $\text{Sr}_2\text{NaNb}_5\text{O}_{15}$ ceramic compact was sintered at 1150 °C in air atmosphere for 2 h at a heating rate equal to 2.0 °C/min. Relative density equal to 65% of the theoretical density was reached. The sintering of the ceramic compact at low temperature aimed to inhibit grain growth, and by consequence, maintain the average crystallite size

very close to the average crystallite size of the nanopowder. In practice, the development of large domains and further interaction between them is blocked. In this sense, an additional contribution to the dielectrical properties stemming from the cooperative phenomenon assigned to large domains is avoided.

Dielectric measurements were carried out by impedance spectroscopy. Platinum electrodes were deposited on both faces of the sample by platinum paste coating (TR-7905 –Tanaka). After complete solvent evaporation, the sample was dried at 800 °C for 30 min. Measurements were taken in the frequency range of 5 Hz to 13 MHz, with an applied potential of 500 mV, using an Impedance Analyzer Alpha N High Resolution Dielectric, Novocontrol GmbH, controlled by a personal computer. The sample was placed in a sample holder with a two-electrode configuration. The measurements were taken from room temperature to 680 °C in 50 °C steps at a heating rate equal to 1.0 °C/min in air atmosphere. A 30-min. interval was used prior to thermal stabilization after before each measurement.

The complex dielectric permittivity, $\varepsilon^*(\omega)$, can be derived from impedance data $Z^*(\omega)$ by the following relations:

$$\varepsilon^*(\omega) = (j\omega C_0 Z^*)^{-1} = \varepsilon'(\omega) - j\varepsilon''(\omega) \quad (\text{A})$$

where $\varepsilon'(\omega)$ and $\varepsilon''(\omega)$ represent the real and imaginary parts of the permittivity and C_0 is the vacuum capacitance. Both parameters $\varepsilon'(\omega)$ and $\varepsilon''(\omega)$ were extracted from impedance in a conventional way, according to the following equations:

$$\varepsilon'(\omega) = Z'' / (2\pi f \varepsilon_0 A |Z|^2) \quad (\text{B})$$

$$\varepsilon''(\omega) = Z' / (2\pi f \varepsilon_0 A |Z|^2) \quad (\text{C})$$

where A represents the geometric factor given by relation S/l , and $|Z|^2$ represents the impedance modulus.

Data were analyzed using the “Equivalent Circuit” (Equivcrt) program ⁽⁹⁾. This one works in an environment developed for equivalent circuits and it is based on the

simulation of impedance spectra data fitted to the experimental diagram. However, this procedure of data analysis is improper, when impedance diagram is incomplete. In this case, the electrical response of the sample displays a high resistive behavior as occurs at around room temperature, when the response of the sample can be regarded as mostly dielectric and the recorded impedance is purely imaginary. In this case, a typical theoretical adjust process of data via equivalent electrical circuits is inadequate to determine the capacitance (dielectric permittivity), since it leads to a gross error. Then, an alternative approach to extract the dielectric permittivity⁽¹⁰⁾ can be used considering the electrical response in a high frequency range from 10^5 to 10^7 Hz, using Equation (D):

$$-\text{Im}(Z) = \frac{1}{jC \omega} \quad (\text{D})$$

where $-\text{Im}(Z)$ is the opposite of the imaginary part of the impedance (Z), j is the complex operator and ω is the angular frequency ($\omega = 2\pi f$). Considering equation (D), the capacitance of the sample, C , is given by the slope of the straight line determined by the variation of $-\text{Im}(Z)$ as a function of $1/2\pi f$. Figure 3 shows as example the variation of $-\text{Im}(Z)$ as a function of $1/\omega$ of the $\text{Sr}_2\text{NaNb}_{15}\text{O}_5$ ceramic at 363 °C.

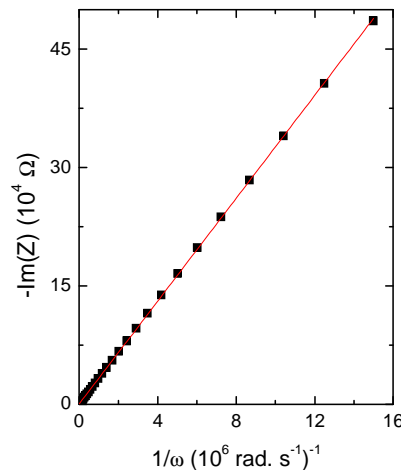


Figure 3. Variation of $-\text{Im}(Z)$ as a function of $1/\omega$ of the $\text{Sr}_2\text{NaNb}_{15}\text{O}_5$ ceramic at 363 °C.

Since the capacitance (C) was determined the dielectric permittivity, ϵ , can be derived from Equation (E):

$$\epsilon = \frac{C}{\epsilon_0} \times \frac{l}{A} \quad (E)$$

where ϵ_0 is the vacuum permittivity, l the thickness of the sample and A the electrode area.

RESULTS AND DISCUSSION

Figure 4 shows the dielectric permittivity curve of $\text{Sr}_2\text{NaNb}_5\text{O}_{15}$ as a function of temperature, calculated from (D) and (E) equations.

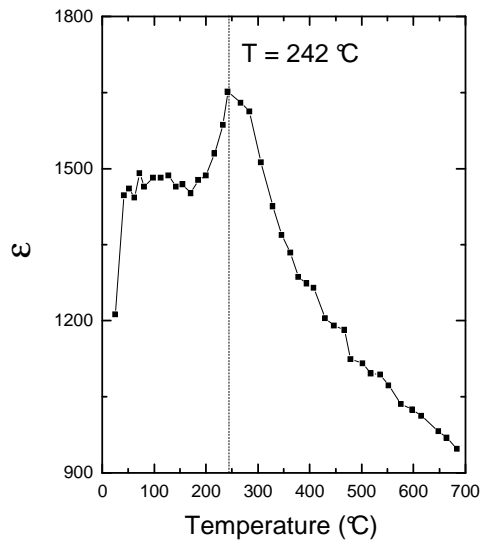


Figure 4. Permittivity curve, ϵ , as a function of temperature of $\text{Sr}_2\text{NaNb}_5\text{O}_{15}$.

The permittivity curve of $\text{Sr}_2\text{NaNb}_5\text{O}_{15}$ shows a set of anomalies of small intensity occurring in shoulder form at around 25 °C and 170 °C and a strong and broad polarization peak of high intensity at 242 °C, with permittivity value equal to 1650. Typically, these anomalies are assigned to phase transitions. Strong anomalies have been assigned to phase transition involving symmetry change, while anomalies of small magnitude have been considered to stem from transitions correlated to the space group ⁽¹¹⁾. The maximum permittivity was previously assigned to the Curie's temperature ($T_C = 245$ °C) of $\text{Sr}_2\text{NaNb}_5\text{O}_{15}$ ⁽¹²⁾. In niobates of perovskite type structure, a defined or diffuse peak at permittivity curve as a function of temperature have been assigned to the structural phase transition or to a set of first-order transitions. Here, the tetragonal symmetry of $\text{Sr}_2\text{NaNb}_5\text{O}_{15}$ seems be invariant in the temperature range investigated due to the high structural anisotropy. For completeness, anomalies have been reported at temperatures higher than 340 °C ⁽¹²⁾.

Figure 5 shows the reciprocal permittivity $1/\varepsilon'$ as a function of temperature. Instead of a single experimental curve, the experimental curve allows to determine two non-parallel linear regions. Each gives a particular Curie's temperature value by extrapolation ($1/\varepsilon' \rightarrow 0$). The first curve gives rise to a "Curie's temperature" equal to 240 °C, a value very close to that reported elsewhere ⁽¹¹⁾. However, the second curve plotted from points above 340 °C leads to a "Curie's temperature" equal to -40 °C. As a matter of fact, one of the already mentioned Curie's temperatures is an apparent value originated from a particular structural evolution as a function of temperature. We can determine the true value by keeping in mind that the value of the displacement of niobium from the center of the octahedron was previously determined.

From the displacement of niobium from the octahedron center, Δz . The spontaneous polarization, P_s , of the $[\text{NbO}_6]$ octahedra depends on the magnitude of the displacement Δz , which is equal to 0.105 Å for the $\text{Sr}_2\text{NaNb}_5\text{O}_{15}$. The value of Curie's temperature can be derived from the empirical equation ⁽¹³⁾:

$$T_C = (2.00 \pm 0.09) \times 10^4 (\Delta z)^2 K \quad (\text{F})$$

The Curie's temperature of $\text{Sr}_2\text{NaNb}_5\text{O}_{15}$ derived by equation (F) is equal to -44°C . This value is in excellent accordance with that derived from the permittivity curve (Fig. 5), which is equal to -40°C .

Based on the above discussion, the first value of Curie's temperature, which is equal to 240°C , is only an apparent value. In this sense, the determination of Curie's temperature by direct inspection of the permittivity versus temperature curve is an imprecise procedure. At this point, we can highlight that $\text{Sr}_2\text{NaNb}_5\text{O}_{15}$ exhibits a real paraelectric state only at temperatures higher than 340°C . Here it is interesting to comment that phase transition temperature can be influenced by lattice stress and/or strain phenomena ⁽¹⁴⁾. Furthermore, the crystallite size can affect the domain size and a lower or higher effect of cooperation between domains can also modify the phase transition temperature or Curie's temperature ⁽¹³⁾.

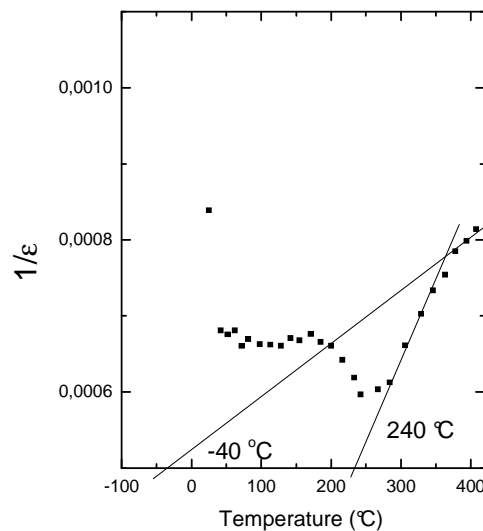


Figure 5. Reciprocal permittivity, $1/\epsilon'$, as a function of temperature.

Figure 6 shows the evolution of the $\epsilon'(\omega)$ and $\epsilon''(\omega)$ parameters obtained from equations (B) and (C), respectively, as a function of frequency at several temperatures. A dispersion in the real permittivity curve $\epsilon'(\omega)$ (Fig. 6a), at low frequency domain ($< 1\text{ KHz}$), is observed with the temperature increasing. In general, these dispersions, normally observed in linear dielectric, are associated to a conduction mechanism ⁽¹⁵⁾.

At high frequency (>1 kHz) the permittivity showed independent of the frequency. None peak was observed in the real permittivity curve $\epsilon'(\omega)$, in all frequency investigated, indicating absence of specific polarization phenomenon, as dipole polarization.

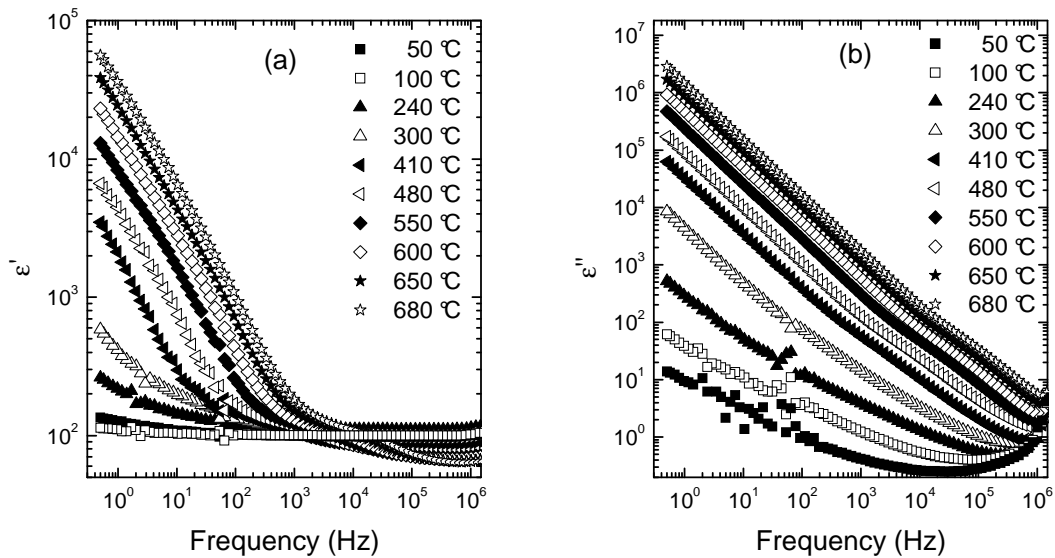


Figure 6. Evolution of the (a) $\epsilon'(\omega)$ and (b) $\epsilon''(\omega)$ parameters as a function of frequency at several temperatures.

The imaginary permittivity curve $\epsilon''(\omega)$ as a function of frequency (Fig. 6b) shows a decreasing of magnitude with frequency increase, in all temperature. High $\epsilon''(\omega)$ values are observed with the temperature increasing at low frequencies. The dispersion degree of the imaginary permittivity decreases to frequency higher than 1 kHz. In all frequency range investigated peaks related to the polarization phenomenon not was observed, in the $\epsilon'(\omega)$ and $\epsilon''(\omega)$ curves of the $\text{Sr}_2\text{NaNb}_5\text{O}_{15}$ solid solution.

CONCLUSION

Modified Polyol method is a suitable method of preparation of niobate nanocrystalline and single phase nanopowders with $\text{Sr}_2\text{NaNb}_5\text{O}_{15}$ TTB-type structure. Due to the very high anisotropy of the crystalline lattice and specific sequence of phase transitions, an apparent Curie's temperature value is generated. The true Curie's temperature is assigned from the displacement of niobium from the octahedron coordination center.

ACKNOWLEDGMENTS

FAPESP, CNPq, and Fundunesp for the financial support.

REFERENCES

- (1) KARAKI, T. *et al.* Growth and optical properties of ferroelectric $\text{K}_3\text{Li}_2\text{Nb}_5\text{O}_{15}$ single crystals. **Japan Journal Applied Physics**, v. 37, p. 5277, 1998.
- (2) KOLAR, D.; GABERSCEK, S.; STADLER, Z.; SUVOROV, D. High stability, low loss dielectrics in the system $\text{BaO-Nd}_2\text{O}_3\text{-TiO}_2\text{-Bi}_2\text{O}_5$, **Ferroelectrics**, v. 27 p. 269, 1980.
- (3) HOU, Y.D.; ZHU, M.K.; TIAN, C.S.; YAN, H. Structure and electrical properties of PMZN–PZT quaternary ceramics for piezoelectric transformers, **Sensors and Actuators A**, v. 116, p. 455, 2004.
- (4) SIMON, A., RAVEZ, J. Solid-state chemistry and non-linear properties of tetragonal tungsten bronzes materials. **Comptes Rendus Chimie**, v. 9, p. 1268-1276, 2006.
- (5) ABRAHAMS S.C.; JAMIESON, P.B.; BERNSTEIN, J.L. Ferroelectric Tungsten Bronze-Type Crystal Structures. III. Potassium Lithium Niobate $\text{K}_{(6-x-y)}\text{Li}_{(4+x)}\text{Nb}_{(10+y)}\text{O}_{30}$, **J. Chem. Phys.**, v. 54, p. 2355, 1971.

- (6) HORNEBECQ, V.; ELISSALDE, C.; WEILL, F.; VILLESUZANNE, A.; MENTRIER, M.; RAVEZ, J. Study of disorder in a tetragonal tungsten bronze ferroelectric relaxor: a structural approach, **J. Appl. Cryst.**, v.33, p. 1037, 2000.
- (7) M. P. Pechini, U.S. pat., No. 3.330.697, 1967.
- (8) LANFREDI, S.; CARDOSO, C. X.; NOBRE, M. A. L. Crystallographic properties of $\text{KSr}_2\text{Nb}_5\text{O}_{15}$. **Materials Science and Engineering B**, v. 112, p. 139–143, 2004.
- (9) BOUKAMP, B. A. - Equivalent circuit - EQUIVCRT Program – Users manual, v. 3, University of Twente-Holand, Enschede, 97 p., 1989.
- (10) NOBRE, M. A. L.; LANFREDI, S. Phase transition in sodium lithium niobate polycrystal: an overview based on impedance spectroscopy. **Journal Physics and Chemistry of Solids**, v. 62, p. 1999-2006, 2001.
- (11) LINES, M.; GLASS, A. Principles and Applications of Ferroelectrics and Related Materials. Oxford, London, (1977).
- (12) GARCÍA, G.E.; TORRES, P.A.; JIMENEZ, R., GONZALEZ, C.J.M. Structural Singularities in Ferroelectric $\text{Sr}_2\text{NaNb}_5\text{O}_{15}$. **Chem. Mater**, v. 19, p. 3575-3580, 2007.
- (13) JAMIESON, P.B.; ABRAHAMS, S.C.; J BRENSTEIN, L. Ferroelectric Tungsten Bronze-Type Crystal Structures. II. Barium Sodium Niobate $\text{Ba}_{(4+x)}\text{Na}_{(2-2x)}\text{Nb}_{10}\text{O}_{30}$, **J. Chem. Phys**, v. 50, p. 4352, 1969.
- (14) GAO, X; XUE, J.; YU, T.; SHEN, Z.; WHANG, J. B-site order-disorder transition in $\text{Pb}(\text{Mg}_{1/3}\text{Nb}_{2/3})\text{O}_3$ - $\text{Pb}(\text{Mg}_{1/2}\text{W}_{1/2})\text{O}_3$ triggered by mechanical activation, **J. Am. Ceram. Soc.**, v. 85, p. 833, 2002.
- (15) NOBRE, M. A. L.; LANFREDI, S. Dielectric spectroscopy on $\text{Bi}_3\text{Zn}_2\text{Sb}_3\text{O}_{14}$ ceramic: an approach based on the complex impedance. **Journal Physics and Chemistry of Solids**, v. 64, p. 2457-2464, 2003.